



Published in final edited form as:

Brain Struct Funct. 2018 July ; 223(6): 2685–2698. doi:10.1007/s00429-018-1652-y.

Paraventricular hypothalamic and amygdalar CRF neurons synapse in the external globus pallidus

Albert J. Hunt Jr^{1,4}, Rajan Dasgupta^{2,4}, Shivakumar Rajamanickam¹, Zhiying Jiang¹, Michael Beierlein^{2,4}, C. Savio Chan³, and Nicholas J. Justice^{1,4}

¹The Brown Foundation Institute of Molecular Medicine for the Prevention of Human Diseases, Center for Metabolic and Degenerative Diseases, University of Texas Health Science Center at Houston, Houston, Texas 77030, USA

²Department of Neurobiology and Anatomy, McGovern Medical School, Houston, Texas 77030, USA

³Department of Physiology, Feinberg School of Medicine, Northwestern University, Chicago, Illinois 60611, USA

⁴Graduate Program in Neuroscience, The University of Texas MD Anderson Cancer Center UTHHealth Graduate School of Biomedical Sciences, Houston, Texas 77030, USA

Abstract

Stress evokes directed movement to escape or hide from potential danger. Corticotropin Releasing Factor (CRF) neurons are highly activated by stress, however, it remains unclear how this activity participates in stress-evoked movement. The external Globus Pallidus (GPe) expresses high levels of the primary receptor for CRF, CRFR1, suggesting the GPe may serve as an entry point for stress-relevant information to reach basal ganglia circuits, which ultimately gate motor output. Indeed, projections from CRF neurons are present within the GPe, making direct contact with CRFR1 positive neurons. CRFR1 expression is heterogenous in the GPe; prototypic GPe neurons selectively express CRFR1 while arkypallidal neurons do not. Moreover, CRFR1 positive GPe neurons are excited by CRF via activation of CRFR1, while nearby CRFR1 negative neurons do not respond to CRF. Using monosynaptic rabies viral tracing techniques, we show that CRF neurons in the stress-activated Paraventricular Nucleus of the Hypothalamus (PVN), Central Nucleus of the Amygdala (CeA), and Bed Nucleus of the Stria Terminalis (BST) make synaptic connections with CRFR1 positive neurons in the GPe, an unprecedented circuit connecting the limbic system with the basal ganglia. CRF neurons also make synapses on Npas1 neurons, although the majority of Npas1 neurons are arkypallidal and do not express CRFR1. Interestingly, prototypic and arkypallidal neurons receive different patterns of innervation from CRF-rich nuclei. Hypothalamic CRF neurons preferentially target prototypic neurons, while amygdalar CRF neurons preferentially target arkypallidal neurons, suggesting that these two inputs to the GPe may

Corresponding author: Nicholas J. Justice, Nicholas.J.Justice@uth.tmc.edu, Phone: (713) 500-3665.

The authors declare no conflicts of interest.

Author Contributions

A.J.H. and N.J.J. designed experiments and analyzed the results; R.D. and M.B. designed and R.D. performed electrophysiological recordings. A.J.H., S.R. and Z.Y. performed immunohistochemical and viral tracing experiments; A.J.H., C.S.C. and N.J.J. wrote the manuscript.

have different impacts on GPe output. Together these data describe a novel neural circuit by which stress-relevant information carried by the limbic system signals in the GPe via CRF to influence motor output.

Keywords

CRF; CRH; CRFR1; CRHR1; Globus Pallidus; Stress

Introduction

Stress and anxiety have profound effects on movement, from the lack of motivation associated with depression, to impacts on coordination in the face of extreme pressure, or the drive to escape or hide from a predator (Heinrichs and Koob, 2004; Lowry and Moore, 2006; Vine et al., 2016). These influences of stress on motor output imply that limbic circuits that are central to the expression of anxiety-related and emotional responses, interact with circuits in the basal ganglia that control execution of motor behaviors (Mogenson et al., 1980; Phelps et al., 2001; Marchand, 2010). The entry point to the basal ganglia for limbic, emotional information has been proposed to be the Nucleus Accumbens (NAcc) given the strong connections between the amygdala and NAcc, as well as its central role in producing reward behavior (Mogenson et al., 1980; Jackson and Moghaddam, 2001).

Mounting evidence suggests that the external Globus Pallidus (GPe), a nucleus that is part of “indirect pathway” basal ganglia circuits, participates in the production of anxiety-related and emotional states. Lesions of the GPe produce anhedonia, depression, auditory hallucinations, anxiety, and paranoia in humans, and the GPe is reduced in size in patients with mood disorders (Lauterbach et al., 1994, 1997; Baumann et al., 1999; Miller et al., 2006). Injection of the GABA-A-receptor antagonist bicuculline in specific regions of the GPe produces anxiety-related behaviors such as stereotypy, attention deficit, and compulsive behavior in non-human primates (Grabli, 2004). In addition, GPe neural firing patterns correlate with reward prediction, suggesting these neurons are sensitive to positive valence (Arkadir et al., 2004; Parush et al., 2008). Although these findings point to a role for the GPe in the expression of anxiety-related behaviors and emotional states, it remains unclear how the GPe interfaces with limbic circuits that carry anxiety and emotionally salient information.

The GPe expresses high levels of the stress neuropeptide receptor, Corticotropin Releasing Factor Receptor type 1 (CRFR1; Van Pett et al., 2000; Justice et al., 2008; Sztainberg et al., 2011). Stress activates a core neural circuitry termed the central autonomic system, in which release of the neuropeptide Corticotropin Releasing Factor (CRF) drives endocrine, autonomic, and behavioral responses (Vale et al., 1981; Swanson et al., 1983; Tazi et al., 1987; Heinrichs et al., 1995; Saper, 2002). The presence of CRFR1 in the GPe suggests that CRF is released in the GPe to influence movement during a stress response (Van Pett et al., 2000; Justice et al., 2008; Sztainberg et al., 2011). Loss of function experiments suggest that CRF has an anxiolytic function in the GPe, in contrast to an anxiogenic function in most other brain regions (Smith et al., 1998; Müller et al., 2003; Sztainberg et al., 2011).

However, these experiments did not take into account the heterogeneity of neuron types of the GPe (Mallet et al., 2012; Abdi et al., 2015; Dodson et al., 2015; Hernández et al., 2015). Not only do subtypes of GPe neurons arise by different lineages, they project to unique targets in the basal ganglia (Flandin et al., 2010; Glajch et al., 2016; Hegeman et al., 2016; Saunders et al., 2016). Given this additional complexity, it is possible that CRF acts on individual GPe cell types to selectively influence motor responses to stress. However, precisely how stress and CRF influences GPe activity to control anxiety-related behavior remains unclear. Here, we show that CRFR1 is expressed on specific GPe neuron classes, that CRF activates CRFR1 positive neurons in the GPe, and that CRF neurons in key stress-responsive nuclei project to and synapse in the GPe.

Materials and Methods

Animal care and genetic crosses

Mice were housed up to five per cage with *ad libitum* access to food and water in a pathogen-free facility with a 12h light/dark cycle. All procedures were performed in accordance with the National Institutes of Health guidelines and with the approval of the University of Texas Health Science Center at Houston Institutional Animal Care and Use Committee (IACUC). Male and female mice aged 8–12 weeks were used for viral tracing and immunohistochemistry experiments. Electrophysiological recordings were performed in 4–8 week old animals. Behavioral experiments were performed using 8–12 week old male mice. The BAC transgenic mouse line, CRFR1-GFP, was used to identify CRFR1 expressing neurons for immunohistochemistry and electrophysiological recordings (Justice et al., 2008). A CRFR1-Cre-2A-tdtomato BAC transgenic mouse line was generated using a similar strategy to the CRFR1-GFP BAC transgenic mouse line. Briefly, a BAC (rp23-239f10; Children's Hospital Oakland Research Institute) containing the entire genomic locus of CRFR1 was modified using recombineering (Liu et al., 2003; Chan et al., 2007). A cassette encoding iCre-p2A-tdtomato-PA was inserted in the first exon at the site of the ATG start codon for CRFR1. Modified BAC DNA was purified and injected in single-celled oocytes to generate transgenic offspring (Genetically Engineered Mouse Core, Baylor College of Medicine, Houston). Three independent transgenic lines were recovered, of which one (CRFR1-Cre) had the best co-localization of Cre/tdtomato with CRFR1-GFP. *In situ* hybridization was performed and confirmed that iCre is expressed in the same cells as Crfr1 in the GPe (Fig. S1A–C). CRFR1-Cre mice were used for viral tracing and behavioral experiments. The BAC transgenic Npas1-iCre-2A-tdtomato mouse line herein referred to as Npas1-Cre has been previously characterized and validated (Hernández et al., 2015). CRH-IRES-Cre (CRF-Cre; Taniguchi et al., 2011; Chen et al., 2015) was obtained from Jackson Laboratories and crossed to a floxed-stop ^{td}Tomato reporter line (Ai9; Madisen et al., 2010) to express ^{td}Tomato in CRF neurons.

Tissue preparation, immunohistochemistry, and cell quantification

Mice were deeply anesthetized by i.p. injection of tribromoethanol (125 mg/kg from a stock solution of 1.25% v/v) and transcardially perfused with saline followed by 4% paraformaldehyde. Brains were removed and post-fixed in the same fixative for 12 h at 4°C. Brains were then equilibrated in 30% sucrose, and 30 µm coronal sections were prepared

using a frozen sliding microtome. Free-floating sections were washed in PBS and incubated overnight in antibodies diluted in PBS + 0.4% Triton X-100 with 2% normal donkey serum. The following antibodies along with notations and citations that validate their accuracy, were used: goat anti-GFP (1:1000, Rockland), does not have any signal when GFP is not present. Rabbit anti-tdTomato (anti-RFP, 1:1000, Abcam, 34771) displays no staining when transgenic tdTomato protein is not present. Rabbit anti-Nkx2.1 (also known as TTF-1; 1:1000, EMD Millipore, 07-601) detects a single band of 42kD by western blot, and has been validated extensively by Millipore for use in immunofluorescent labeling (antibody originally made by Upstate). Mouse anti-Parvalbumin (1:1000, EMD Millipore, MAB1572) detects a single band of 12kD on a western blot and colocalizes with multiple transgenic reporters of parvalbumin expression. Rabbit anti-Npas1 (Npas1, 1:1000, Chan lab) was generated in the Chan lab and validated by demonstrating the lack of staining in Npas1 null mutant mice (Hernández et al. 2015). Rabbit anti-FoxP2 (1:1000, EMD Millipore, ABE73) recognizes a major band of the correct size (~80kD) on a western blot and has been used extensively in previous publications to recognize FoxP2 neurons in the GPe (Hernández et al. 2015), Mouse anti-SV2 (mouse monoclonal SV2, 1:1000, Developmental Studies Hybridoma Bank) recognizes all three isoforms of the SV2 protein (SV2, A, B, C) and was validated by electron microscopy, immunohistochemistry, and western blot when originally published (Buckley and Kelly 1985). Rabbit anti-CRF (rc70, 1:2000, gift from W. Vale, The Salk Institute), which was created by the Vale lab by injecting purified CRF into rabbits, has been validated extensively (Swanson et al. 1983; Chen et al. 2015). Goat anti-CRFR1 (Everest Biotech, 1:100, EB07553, lot. G2) recognizes a single band at ~60kD on a western blot, and does not detect protein in mice lacking CRFR1 (T. Baram pers com; Jüngling et al. 2012). It is important to note that we and others have used other lots of this particular antisera and have observed minimal labeling (Refojo, et al., 2011). Following incubation, tissue sections were washed in PBS and treated with the appropriate secondary antibody for 2 h, washed in PBS, and mounted on gelatin-coated slides. Images were obtained on a Leica TCS SP5 confocal microscope. In CRFR1-GFP mice, colocalization of GFP and the molecular marker of interest was quantified by manual counting of 3 images per brain from three to five mice at different rostrocaudal levels of the GPe. Quantification was averaged over all sections. For tracing experiments, every fourth section was mounted for quantification of starter and traced cells using an epifluorescent microscope.

Stereotaxic injections

Mice were deeply anesthetized with isoflurane and secured in a mouse stereotaxic frame. Under aseptic conditions, an incision was made to expose the skull. Bilateral craniotomies were made using a drill at coordinates 0.0 mm rostral, \pm 2.1 mm lateral of Bregma. Injections were made at -3.8 mm ventral to bregma using a Nanoject II (Drummond Scientific) with a pulled glass pipette, at a rate of 50 nl/min. Following completion of each injection, the pipette was left in place for 5 minutes to allow for absorption of the virus before being removed. For viral tracing, we injected 50 nl of a 1:1 mixture of Cre-dependent AAVs carrying FLEXed TVA-mCherry and FLEXed Rabies G (AAV-EF1a-FLEX-TVA-mCherry, AAV-CA-FLEX-G obtained from the UNC viral vector core; Watabe-Uchida et al., 2012). After 2 weeks, we delivered 200 nl of pseudotyped rabies virus (AAV-EnvA-SAD G-eGFP supplied by Dr. Ben Arenkiel; Wickersham et al., 2007) in the same location.

After 5 days we made an i.c.v. injection of colchicine (0.3 mg/kg solution in ddH₂O) to enhance CRF staining of cell bodies. Mice were sacrificed at 7 days after injection of PTRV. For retrograde tracing with fluorescent beads, mice were injected with 150 nl per side, Alexa-555 conjugated beads (Lumafluor Inc) at the identical coordinates used for the GPe in tracing studies. Mice were sacrificed 7 days after injection and prepared for histology as above.

Slice preparation

Parasagittal slices (250 μ m) were obtained from male and female CRFR1-GFP mice, aged P35–53. Animals were anesthetized using isoflurane, decapitated, and their brains were quickly extracted and placed into ice-cold solution saturated with 95% O₂–5% CO₂, and consisting of the following (in mM): 212 sucrose, 2.5 KCl, 1.25 NaH₂PO₄, 10 MgSO₄, 26 NaHCO₃, 11 glucose, and 0.5 CaCl₂. Slices were prepared using a vibratome (Leica VT1200S) and then incubated at 34°C for 50 min in artificial cerebrospinal fluid (ACSF) containing the following (in mM): 126 NaCl, 26 NaHCO₃, 2.5 KCl, 1.25 NaH₂PO₄, 10 glucose, 2 CaCl₂, and 1 MgCl₂ (saturated with 95% O₂–5% CO₂). Slices were then kept at room temperature until used for experiments.

Electrophysiological recordings

Recordings were performed at 31–33°C using an in-line heater (Warner Instruments) while perfusing the recording chamber with ACSF. Neurons were visualized using infrared differential interference contrast using an Olympus BX51WI microscope and a video camera (IR-1000 Dage-MTI). GFP+ cells were identified under epifluorescence using an X-Cite 120Q light source. Loose-patch voltage-clamp recordings from CRFR1-GFP+ and GFP–GPe neurons were obtained with glass pipettes (3–5 M Ω) filled with ACSF. Seal resistance was maintained between 40–70 M Ω . To minimize perturbations of the firing rate of the recorded neuron, command voltage was continuously adjusted during the recordings to maintain a holding current near 0 pA (Perkins, 2006). Experiments were done in the presence of DNQX (10 μ M), D-APV (25 μ M), and Picrotoxin (50 μ M) to block AMPARs, NMDARs, and GABAARs, respectively. DNQX, Antalarmin, Picrotoxin and D-APV were obtained from R&D Systems. CRF was kindly provided by J. Rivier (Salk Institute). All other chemicals were obtained from Sigma-Aldrich.

Data acquisition and analysis

Data were acquired using an amplifier (Multiclamp 700B; Molecular Devices), filtered at 6–10 kHz, and digitized at 20 kHz with a 16-bit analog-to-digital converter (Digidata 1440A; Molecular Devices). Recordings were acquired using Clampex 10.3 software (Molecular Devices) and analyzed using custom macros written in Igor Pro (Wavemetrics).

Statistics

All data are presented as the mean \pm SEM, and the statistical analyses were done with Graphpad Prism 5.04. In CRFR1-GFP mice, colocalization of GFP and the molecular marker of interest was quantified by manual counting of 3 images per brain from three to five mice at different rostrocaudal levels of the GPe. For tracing experiments, one quarter of

the brain sections were mounted for quantification of starter and traced cells using an epifluorescent microscope. Two-tailed unpaired student's t-tests were used to compare the connectivity ratios of CRFR1 positive neurons and Npas1 positive neurons.

Results

CRF neurons project to the GPe

The GPe expresses high levels of CRFR1, however, CRF neuron projections to the basal ganglia, and CRF effects on neuronal excitability in the GPe have not been systematically examined (Van Pett et al., 2000; Justice et al., 2008; Sztainberg et al., 2011). To visualize CRF neuron projections to the GPe, we imaged sections of the GPe from CRFR1-GFP; CRF-cre; floxed-stop^{td}Tomato mice (Fig. 1). CRFR1-GFP mice have been validated for expression of GFP in neurons that express CRFR1 in the GPe by *in situ* hybridization (Justice et al., 2008; Sztainberg et al., 2011), and by co-immunolocalization of CRFR1 protein with GFP in CRFR1-GFP transgenic mice (Fig. S1D–F). In addition, the CRF-IRES-Cre; floxed-stop^{td}Tomato mouse line has been shown to express Cre accurately in neurons that express CRF (Taniguchi et al., 2011; Chen et al., 2015). In sections of the GPe from mice carrying all three transgenes, CRFR1 neurons are labeled with GFP and projections from CRF neurons are labeled with ^{td}Tomato (Fig. 1). ^{td}Tomato positive fibers from CRF neurons are evident within the GPe at all rostrocaudal levels (Fig. 1A, D, G). Although CRF innervation of the GPe was present in all regions of the GPe, the ventral portions of the GPe consistently displayed denser projections from CRF neurons (Fig. 1). Co-labeling for the presynaptic marker SV2 reveals putative synaptic contacts between CRF neuron axonal fibers (^{td}Tomato positive) and CRFR1-GFP positive dendrites and cell bodies (Fig. 1, right column). Immunofluorescent labeling for CRF peptide reveals that many tomato positive projections contain CRF, suggesting that CRF is released in the GPe (Fig. S2).

CRFR1 is expressed by prototypic neurons in the GPe

The GPe has recently been shown to contain heterogeneous cell types that arise from distinct neural lineages and have differing afferent and efferent connections (Mallet et al., 2012; Abdi et al., 2015; Dodson et al., 2015; Hernández et al., 2015; Glajch et al., 2016). Neurons derived from the medial ganglionic eminence that express Nkx2.1 and/or Parvalbumin (PV) and project primarily to the subthalamic nucleus are termed “prototypic” (Nóbrega-Pereira et al., 2008; Flandin et al., 2010; Mallet et al., 2012; Hernandez et al., 2015; Glajch et al., 2016; Hegeman et al., 2016). Neurons derived from the lateral ganglionic eminence that express the transcription factors FoxP2 and Npas1 and project to the dorsal striatum and are termed “arkypallidal” (Nóbrega-Pereira et al., 2008; Flandin et al., 2010; Mallet et al., 2012; Hernandez et al., 2015; Glajch et al., 2016; Hegeman et al., 2016). To determine which classes of neurons in the GPe express CRFR1, we performed immunofluorescence labeling using GPe cell markers in CRFR1-GFP mice. In the GPe, CRFR1-GFP is expressed by $60.1 \pm 4.7\%$ of GPe neurons (Fig. 2Q). Of these, $86.0 \pm 5.2\%$ of CRFR1-GFP positive neurons co-express Nkx2.1 (Fig. 2A–C, R), while $72.6 \pm 0.9\%$ of Nkx2.1 positive neurons co-express GFP (Fig. 2S). A subpopulation of Nkx2.1 positive GPe neurons express parvalbumin (PV; Abdi et al., 2015; Hernández et al., 2015). $53.3 \pm 3.2\%$ of the CRFR1-GFP positive neurons in the GPe express PV (Fig. 2D–F, R). Moreover, $36.3 \pm 2.4\%$ of

CRFR1-GFP positive neurons express both Nkx2.1 and PV (Fig. 2M–P). Nearly all ($98.6 \pm 0.4\%$) PV neurons express CRFR1-GFP, consistent with previous reports (Sztainberg et al., 2011). We find that no CRFR1-GFP positive neurons express the arkypallidal neuron marker FoxP2 (Fig. 2J–L; Abdi et al., 2015; Dodson et al., 2015). However, a small population of CRFR1-GFP positive neurons express Npas1 ($6.5 \pm 1.1\%$, Fig. 2G–I). While most Npas1 positive neurons are arkypallidal, CRFR1-GFP positive/Npas1 positive neurons are not arkypallidal neurons because they do not express FoxP2 (Mallet et al., 2012; Hernández et al., 2015). Finally, CRFR1 is expressed by cholinergic neurons in the GPe (not shown). Given the expression pattern of these GPe cell type markers, we conclude that CRFR1 is predominantly expressed by prototypic neurons in the GPe.

CRF increases the activity of CRFR1 positive GPe neurons

To investigate the impact of CRF on GPe neuron excitability, we prepared brain slices from CRFR1-GFP mice and performed simultaneous loose-patch recordings from neighboring GFP positive cells and GFP negative cells in the GPe. We blocked fast glutamatergic and GABAergic synaptic transmission with $10 \mu\text{M}$ DNQX, $25 \mu\text{M}$ AP5, and $50 \mu\text{M}$ Picrotoxin to examine the effects of CRF on the autonomous activity of GPe neurons. Following bath application of 30 nM CRF, GFP positive GPe neurons displayed a significant increase in mean firing rate (from $25.8 \pm 8.9 \text{ Hz}$ to $47.6 \pm 6.1 \text{ Hz}$, $n = 5$, $t(4)=2.88$, $p<0.05$, Fig. 3A, green trace) while simultaneously recorded GFP negative GPe neurons were unaffected by the application of CRF ($12.0 \pm 3.9 \text{ Hz}$ vs. $12.4 \pm 3.9 \text{ Hz}$ $n=5$, $t(4)=0.34$, $p=0.75$, Fig. 3A, grey trace). To ensure that the observed response to CRF in GFP positive GPe neurons was mediated by CRFR1, we recorded from GFP positive GPe neurons in the presence of the selective CRFR1 antagonist Antalarmin (Webster 1996). In the presence of $1 \mu\text{M}$ Antalarmin, CRF application does not increase the mean firing rate of CRFR1-GFP neurons ($21.99 \text{ Hz} \pm 7.61 \text{ Hz}$ vs. $19.02 \pm 6.06 \text{ Hz}$, $t(4)=0.92$, $p=0.41$, Fig. 3B). These data confirm that GFP expression in CRFR1-GFP mice corresponds with functional expression of CRFR1 in the GPe, and that CRFR1 positive GPe neurons are excited by CRF.

Tracing inputs to CRFR1 positive and Npas1 positive GPe neurons

To identify the origin of CRF projections to the GPe, we performed rabies viral tracing from GPe CRFR1 neurons (Wickersham et al., 2007). We made injections of Cre-dependent TVA-mCherry/G encoding AAVs in CRFR1-Cre BAC transgenic mice that express Cre in CRFR1 positive neurons (Fig. 4A; Watabe-Uchida et al., 2012). CRFR1-Cre, which also express ^{td}Tomato from the transgene (iCre-2A-^{td}Tomato) were validated for the expression of Cre in CRFR1 neurons by performing double label *in situ* hybridization their corresponding transcripts (Fig. S1A–C) and by immunostaining for the colocalization of ^{td}Tomato and CRFR1 protein (Fig. S1G–I). All ^{td}Tomato+/Cre neurons in the GPe of these mice were also positive for CRFR1 mRNA/protein, validating this line for use in manipulating CRFR1+ GPe neurons (Fig. S1). Two weeks after helper virus injections, we injected the same coordinates with a pseudotyped rabies virus (PTRV) that expresses GFP (EnvA-SAD G-GFP; Fig. 4A). G-deleted EnvA pseudotyped rabies virus can only infect cells that express TVA, and will only package in the presence of G, thus we infected CRFR1 neurons with rabies virus, and this virus packaged and trans-synaptically infected neurons that synapse on GPe CRFR1 neurons. This strategy normally produced 5–10 “starter” neurons (neurons

competent to generate rabies virus; Fig. 4A) in the GPe. We see no infection with pseudotyped rabies virus in injections of animals that did not receive helper virus injections (Fig. 4B). As CRFR1 is expressed by a small proportion of Npas1 positive neurons, we also traced monosynaptic connections to Npas1 positive GPe neurons using pseudotyped rabies virus in Npas1-Cre mice (Hernández et al., 2015).

The majority of monosynaptically-traced neurons that target CRFR1 or Npas1 GPe neurons reside in the GPe (Fig. 4C) and Striatum (Fig. 4D). We also see neurons in the cortex (Fig. 4E), thalamus (Fig. 4F), hypothalamus, STN (Fig. 4G), SNc (Fig. 4H) and amygdala. We counted the number and location of CRFR1-cre and Npas1-cre starter neurons that were red fluorescent (TVA-mChy puncta) and green fluorescent (SAD G-GFP). We also counted the number and location of all monosynaptically traced neurons that were green fluorescent only (SAD G-GFP) in each experiment. For each mouse we calculated a “connectivity ratio” by taking the ratio of traced neurons in a particular brain region divided by the total number of starter neurons in the GPe to normalize the number of traced cells to the number of starter neurons observed in each experiment. Using this metric, we found that the regions with the highest levels of monosynaptic connectivity to CRFR1 positive and Npas1 positive starter neurons are the GPe and Striatum (Fig. 4I). We also find consistent projection density from the thalamus (mainly parafascicular nucleus), hypothalamus, subthalamic nucleus (STN), Substantia Nigra pars compacta (SNc), amygdala, and cortex (Fig. 4I). Broadly, we saw similar numbers of traced neurons in nuclei projecting to CRFR1-Cre and Npas1-Cre neurons in the GPe (Fig. 4I).

CRFR1 positive and Npas1 positive GPe neurons receive inputs from CRF neurons in the PVN, CeA and BST

Stress responsive nuclei in the hypothalamus, amygdala and BST contain abundant CRF neurons, however projections from these nuclei to GPe have not previously been described. Consistently, when we traced monosynaptic projections to CRFR1 positive GPe neurons, we found labeled neurons in the lateral dorsal region of the Bed nucleus of the stria terminalis (BSTld; Fig. 5A), the paraventricular nucleus of the hypothalamus (PVN; Fig. 5B), and the Central Nucleus of the Amygdala (CeA; Fig. 5C), which are common nuclei of the stress responsive central autonomic system (Saper et al., 2002). We also observed monosynaptically-connected projection neurons in these nuclei when we traced Npas1 neurons, even though the majority of Npas1 positive neurons do not express CRFR1 (Fig. 5D–F). Immunohistochemical labeling for CRF demonstrated that GPe-projecting neurons in each of these regions make CRF (Fig. 5A–F). Of the sections from CRFR1-cre experiments that were stained for CRF, 54.7% (23 out of 42) of traced neurons in the CeAl (lateral subdivision of the CeA), 53.1% (17 out of 32) of traced neurons in the PVN, and 25% (1 out of 4) of traced neurons in the BSTld were positive for CRF peptide (Fig. 5G). From Npas1-Cre experiments sections stained for CRF, 84.2% (16 out of 19) of traced neurons in the CeAl, 66.7% (2 out of 3) traced neurons in the PVN, and 60% (3 out of 5) traced neurons in the BSTld were CRF positive (Fig. 5G). To provide additional evidence for the existence of this novel circuit between the hypothalamus/BST/CeA and the GPe, we injected retrograde tracers (retrobeads) into the GPe of animals carrying CRF-Cre; LSL-L10Agfp transgenes. Again, we observed neurons in the PVN (S2A-C), BSTld (S2D-F), and

CeA (Fig. S2G–I) positively labeled with the retrograde tracer. As observed in the rabies tracing experiments, approximately 50% of retrogradely traced neurons were CRF neurons (Fig. S2).

When we compare the connectivity ratio from stress responsive nuclei between CRFR1-Cre and Npas1-Cre tracing experiments, we find that the CeAl and CeAm (lateral and medial subdivisions of the CeA) are more highly connected with Npas1 neurons than with CRFR1 GPe neurons (Fig. 6H; CeAl: 2.2 ± 0.3 in Npas1-Cre compared to 1.0 ± 0.3 in CRFR1-Cre; $t(9)=2.87$, $p<0.05$; CeAm: 0.9 ± 0.3 in Npas1-Cre compared to 0.1 ± 0.0 in CRFR1-Cre animals; $t(6)=3.18$, $p<0.01$). Conversely, we observed fewer neurons monosynaptically labeled in the PVN when tracing Npas1 GPe neurons compared to CRFR1 GPe neurons, although this result was highly variable between animals (Fig. 6H; 0.5 ± 0.3 vs. 0.1 ± 0.1 ; $t(8)=1.22$, $p=.25$). This differential connectivity with specific stress responsive nuclei suggests that CRFR1 and Npas1 neurons receive CRF and stress related information from different sources, with CRFR1 neurons receiving more inputs from the PVN, and Npas1 neurons receiving more inputs from the amygdala.

Discussion

This study focuses on how stress-relevant information impinges on the basal ganglia via the GPe. In mice, we observe CRF neuron projections in the GPe (Fig. 1). Monosynaptic tracing of afferent connections to specific neural classes in the GPe detects synapses from CRF neurons in the PVN, CeA, and BSTld (Fig. 5). While connections between the amygdala and the Nucleus Accumbens have been considered the most likely route of information flow between limbic and basal ganglia circuits (Mogenson et al., 1980), our current study is the first to report monosynaptic inputs from CRF neurons in the PVN, CeA, and BST to the GPe. These findings open a new route by which limbic circuits interface with the basal ganglia to provide emotional, stress or anxiety relevant information to motor circuits that control movement. The term GPe originally came from the primate anatomical nomenclature, and has become the conventional designation for the rodent Globus Pallidus (Parent and Hazrati, 1995, Kita, 2007, Hegeman, et al., 2016, Gittis, et al., 2014). While we do not imply our findings can be directly translated to primates, our ultimate goal is to be able to inform our understanding in humans.

Cell type specificity

The GPe contains heterogeneous neuronal subtypes (Abdi et al., 2015; Dodson et al., 2015; Hernández et al., 2015; Hegeman et al., 2016) We found that particular classes of neurons in the GPe express CRFR1, and are activated by CRF. CRFR1 is predominantly expressed by Nkx2.1 positive neurons (>85%), with no FoxP2 positive arky pallidal neurons expressing CRFR1. However, a small number of Npas1 positive neurons express CRFR1 (<10%), suggesting that CRF can signal to both Nkx2.1 positive/Npas1 negative prototypic neurons which project to the subthalamic nucleus, and Npas1 positive/CRFR1 positive neurons which project to the dorsal striatum (Abdi et al., 2015; Hernández et al., 2015; Glajch et al., 2016; Saunders et al., 2016). Interestingly, we found that CRFR1 positive neurons and Npas1 positive neurons receive distinct patterns of stress-related inputs, with Npas1 positive

neurons being preferentially targeted by CRF neurons in the CeA (Fig. 5H). Finally, in all three stress-responsive nuclei, we observed neurons that were both positively- and negatively-labeled for CRF that target the GPe (Fig. 5). Given that these nuclei express a diverse array of neuropeptides such as Vasopressin and Oxytocin, it is likely that other neuropeptide neurons, in addition to CRF neurons, project to the GPe. CRF and other neuropeptides released in GPe might control additional behaviors beyond anxiety-related behavior, from feeding to sexual and reproductive behaviors via connections with the GPe (Lim et al., 2004; Chometton et al., 2014; Freeman et al., 2014; Xue et al., 2016).

The nature of CRF synapses in the GPe

We have described a novel projection from CRF neurons in the PVN, CeA and BST to the GPe. These neurons contain CRF (Fig. S2) and likely release CRF to activate prototypic GPe neurons, although we have not directly measured CRF release. PVN CRF neurons can also release glutamate, and CeA CRF neurons release GABA, both of which are released at chemical synapses (Dabrowska et al., 2013; Füzesi et al., 2016). We observed transsynaptic infections of rabies virus between both amygdalar and hypothalamic CRF neurons and GPe neurons, indicating that a tight synapse exists between CRF neurons and their projection targets in the GPe (Ugolini, 1995). In the case of glutamatergic synapses from the PVN, CRF release might serve to potentiate glutamatergic signaling. For GABAergic projections from the amygdala, it is unclear how CRF co-release would impact signaling, given that GABA is inhibitory and CRF is excitatory on GPe neurons (Fig. 3). Further investigation is needed to determine whether CRF is released at a synapse, the nature of fast synaptic connections between PVN and CeA CRF neurons and GPe neurons, and how CRF, signaling as a neuropeptide, modulates fast synaptic signaling in the GPe (Nusbaum et al., 2017).

Stress related symptoms in basal ganglia disorders

Stress related disease has been reported to accompany diseases associated with basal ganglia dysfunction including Parkinson's Disease (Henderson et al., 1992; Lauterbach et al., 2003) and Huntington's disease (Berrios et al., 2002; Duff et al., 2007). In PD, this ranges from anxiety (up to 69%), to depression (~30%) and generalized anxiety disorder (~11%), as the most common neuropsychiatric co-morbidities (Nuti et al., 2004; Kulisevsky et al., 2008; Dissanayaka et al., 2010; Leentjens et al., 2011). These symptoms are thought to arise both from stress associated with disease progression, as well as dysfunction in the underlying circuitry that causes anxiety symptoms (Prediger et al. 2012). Interestingly, the severity of motor symptoms in these diseases often tracks with the intensity of anxiety-related symptoms, suggesting there is a causal relationship between the level of stress and motor dysfunction (Siemers et al., 1993). The GPe is a principal nucleus in basal ganglia motor circuits that dysfunctions in PD and HD (reviewed in Hegeman et al., 2016). CRF signaling to the GPe has the potential to alter patterns of GPe activity that could initiate or exacerbate existing motor dysfunctions caused by underlying basal ganglia pathologies. Indeed, lesions of the GPe produce anhedonia in humans and the GPe is reduced in size in patients with mood disorders (Lauterbach et al., 1994, 1997; Baumann et al., 1999; Miller et al., 2006). It remains to be determined how connections between stress-related circuits and motor circuits contribute to anxiety-related symptoms in the context of basal ganglia dysfunction.

Emotional content and the basal ganglia

Mounting evidence suggests that the basal ganglia has some role in the processing of affective, emotional information, in addition to its well characterized role in gating movement (Mogenson et al., 1980; Marchand, 2010). Most studies have proposed that emotionally relevant information enters the basal ganglia via the NAcc (Mogenson et al., 1980; Jackson and Moghaddam, 2001; Phelps et al., 2001). Here, we show projections from CRF neurons in the amygdala and the PVN, form an unprecedented circuit connecting the amygdala and hypothalamus directly to the GPe. CRF neurons at both of these sites are highly activated by psychologic and physiologic stress, and are well characterized to orchestrate a combined endocrine, autonomic and behavioral response to stress (Vale et al., 1981; Swanson et al., 1983; Chan et al., 1993; Heinrichs et al., 1995). Why do these neurons project to the GPe? We suggest that this projection influences motor output to drive context appropriate escape and freezing behaviors during a stress response, which are differentially regulated by the heterogeneous neural populations that reside in the GPe. In addition, basal ganglia circuits that include the GPe, gate signals arising in the cortex, which may be modulated by inputs from the amygdala and PVN via CRF release in the GPe. While neuronal types in the GPe are intermixed, an emotional GPe circuit may be distinct from circuits that gate motor behavior. Based on the location of traced CRFR1+ or Npas1+ neurons within the GPe, and the location of neurons that make synapses on GPe neurons in structures such as the striatum and subthalamic nucleus, we have not been able to segregate motor and limbic circuitry that transits the GPe. Given these newly discovered inputs from stress-responsive circuits, further investigation is needed to determine the organization of stress responsive GPe circuits and their role in adding emotional salience to the activity of basal ganglia circuits that mediate behavioral output in response to stress.

Supplementary Material

Refer to Web version on PubMed Central for supplementary material.

Acknowledgments

The authors thank Z. Mao who provided expertise in confocal microscopy. We thank L. Mangieri and Q. Tong for their valuable input in data interpretation and resource sharing. We thank J. Selever, A. Herman, and B. Arenkiel for their kind gift of viral preparations necessary to perform tracing experiments. This work was supported in part by National Institute of Neurological Disorders and Stroke Grants NS077989 to M.B., NS069777 and NS047085 to C.S.C., MH112768 to N.J.J and C.S.C., and MH114032 to N.J.J. R.D. was supported by a Zilkha Family Discovery Fellowship in Neuroengineering.

References

- Abdi A, Mallet N, Mohamed FY, Sharott A, Dodson PD, Nakamura KC, Suri S, Avery SV, Larvin JT, Garas FN, Garas SN, Vinciati F, Morin S, Bezaud E, Baufreton J, Magill PJ. Prototypic and arypallidal neurons in the dopamine-intact external globus pallidus. *J Neurosci*. 2015; 35:6667–6688. [PubMed: 25926446]
- Arkadir D, Morris G, Vaadia E, Bergman H. Independent coding of movement direction and reward prediction by single pallidal neurons. *J Neurosci*. 2004; 24:10047–10056. [PubMed: 15537873]
- Baumann B, Danos P, Krell D, Diekmann S, Leschinger A, Stauch R, Wurthmann C, Bernstein HG, Bogerts B. Reduced volume of limbic system-affiliated basal ganglia in mood disorders: preliminary data from a postmortem study. *J Neuropsychiatry Clin Neurosci*. 1999; 11:71–78. [PubMed: 9990559]

- Berrios GE, Wagle AC, Marková IS, Wagle SA, Rosser A, Hodges JR. Psychiatric symptoms in neurologically asymptomatic Huntington's disease gene carriers: a comparison with gene negative at risk subjects. *Acta Psychiatr Scand.* 2002; 105:224–230. [PubMed: 11939977]
- Chan RK, Brown ER, Ericsson A, Kovács KJ, Sawchenko PE. A comparison of two immediate-early genes, c-fos and NGFI-B, as markers for functional activation in stress-related neuroendocrine circuitry. *J Neurosci.* 1993; 13:5126–5138. [PubMed: 8254363]
- Chan W, Costantino N, Li R, Lee SC, Su Q, Melvin D, Court DL, Liu P. A recombineering based approach for high-throughput conditional knockout targeting vector construction. *Nucleic Acids Res.* 2007; 35:e64. [PubMed: 17426124]
- Chen Y, Molet J, Gunn BG, Ressler K, Baram TZ. Diversity of Reporter Expression Patterns in Transgenic Mouse Lines Targeting Corticotropin-Releasing Hormone-Expressing Neurons. *Endocrinology.* 2015; 156:4769–4780. [PubMed: 26402844]
- Chometton S, Cvetkovic-Lopes V, Houdayer C, Franchi G, Mariot A, Poncet F, Fellmann D, Risold P-Y. Anatomical organization of MCH connections with the pallidum and dorsal striatum in the rat. *Front Syst Neurosci.* 2014; 8:185. [PubMed: 25324738]
- Dabrowska J, Hazra R, Guo J-D, Dewitt S, Rainnie DG. Central CRF neurons are not created equal: phenotypic differences in CRF-containing neurons of the rat paraventricular hypothalamus and the bed nucleus of the stria terminalis. *Front Neurosci.* 2013; 7:156. [PubMed: 24009552]
- Dissanayaka NNW, Sellbach A, Matheson S, O'Sullivan JD, Silburn PA, Byrne GJ, Marsh R, Mellick GD. Anxiety disorders in Parkinson's disease: prevalence and risk factors. *Mov Disord.* 2010; 25:838–845. [PubMed: 20461800]
- Dodson PD, Larvin JT, Duffell JM, Garas FN, Doig NM, Kessar N, Duguid IC, Bogacz R, Butt SJB, Magill PJ. Distinct developmental origins manifest in the specialized encoding of movement by adult neurons of the external globus pallidus. *Neuron.* 2015; 86:501–513. [PubMed: 25843402]
- Duff K, Paulsen JS, Beglinger LJ, Langbehn DR, Stout JC. Psychiatric Symptoms in Huntington's Disease before Diagnosis: The Predict-HD Study. *Biol Psychiatry.* 2007; 62:1341–1346. [PubMed: 17481592]
- Flandin P, Kimura S, Rubenstein JLR. The progenitor zone of the ventral medial ganglionic eminence requires Nkx2-1 to generate most of the globus pallidus but few neocortical interneurons. *J Neurosci.* 2010; 30:2812–2823. [PubMed: 20181579]
- Freeman SM, Walum H, Inoue K, Smith AL, Goodman MM, Bales KL, Young LJ. Neuroanatomical distribution of oxytocin and vasopressin 1a receptors in the socially monogamous coppery titi monkey (*Callicebus cupreus*). *Neuroscience.* 2014; 273:12–23. [PubMed: 24814726]
- Füzesi T, Daviu N, Wamsteeker Cusulin JI, Bonin RP, Bains JS. Hypothalamic CRH neurons orchestrate complex behaviours after stress. *Nat Commun.* 2016; 7:11937. [PubMed: 27306314]
- Gittis AH, Berke JD, Bevan MD, Chan CS, Mallet N, Morrow MM, Schmidt R. New roles for the external globus pallidus in basal ganglia circuits and behavior. *J Neurosci.* 2014; 34(46):15178–83. [PubMed: 25392486]
- Glajch KE, Kolver DA, Hegeman DJ, Cui Q, Xenias HS, Augustine EC, Hernández VM, Verma N, Huang TY, Luo M, Justice NJ, Chan CS. Npas1+ Pallidal Neurons Target Striatal Projection Neurons. *J Neurosci.* 2016; 36:5472–5488. [PubMed: 27194328]
- Grabli D. Behavioural disorders induced by external globus pallidus dysfunction in primates: I. Behavioural study. *Brain.* 2004; 127:2039–2054. [PubMed: 15292053]
- Hegeman DJ, Hong ES, Hernández VM, Chan CS. The external globus pallidus: progress and perspectives. *Eur J Neurosci.* 2016; 43:1239–1265. [PubMed: 26841063]
- Heinrichs SC, Koob GF. Corticotropin-releasing factor in brain: a role in activation, arousal, and affect regulation. *J Pharmacol Exp Ther.* 2004; 311:427–440. [PubMed: 15297468]
- Heinrichs SC, Menzaghi F, Merlo Pich E, Britton KT, Koob GF. The role of CRF in behavioral aspects of stress. *Ann N Y Acad Sci.* 1995; 771:92–104. [PubMed: 8597448]
- Henderson R, Kurlan R, Kersun JM, Como P. Preliminary examination of the comorbidity of anxiety and depression in Parkinson's disease. *J Neuropsychiatry Clin Neurosci.* 1992; 4:257–264. [PubMed: 1498578]

- Hernández VM, Hegeman DJ, Cui Q, Kelper DA, Fiske MP, Glajch KE, Pitt JE, Huang TY, Justice NJ, Chan CS. Parvalbumin+ Neurons and Npas1+ Neurons Are Distinct Neuron Classes in the Mouse External Globus Pallidus. *J Neurosci*. 2015; 35:11830–11847. [PubMed: 26311767]
- Jackson ME, Moghaddam B. Amygdala regulation of nucleus accumbens dopamine output is governed by the prefrontal cortex. *J Neurosci*. 2001; 21:676–681. [PubMed: 11160446]
- Justice NJ, Yuan ZF, Sawchenko PE, Vale W. Type 1 corticotropin-releasing factor receptor expression reported in BAC transgenic mice: implications for reconciling ligand-receptor mismatch in the central corticotropin-releasing factor system. *J Comp Neurol*. 2008; 511:479–496. [PubMed: 18853426]
- Kita H. Globus pallidus external segment. *Prog Brain Res*. 2007; 160:111–33. DOI: 10.1016/S0079-6123(06)60007-1 [PubMed: 17499111]
- Kulisevsky J, Pagonabarraga J, Pascual-Sedano B, Gironell A, García-Sánchez C, Martínez-Corral M. Motor changes during sertraline treatment in depressed patients with Parkinson's disease*. *Eur J Neurol*. 2008; 15:953–959. [PubMed: 18637826]
- Lauterbach EC, Freeman A, Vogel RL. Correlates of generalized anxiety and panic attacks in dystonia and Parkinson disease. *Cogn Behav Neurol*. 2003; 16:225–233. [PubMed: 14665822]
- Lauterbach EC, Jackson JG, Price ST, Wilson AN, Kirsh AD, Dever GE. Clinical, motor, and biological correlates of depressive disorders after focal subcortical lesions. *J Neuropsychiatry Clin Neurosci*. 1997; 9:259–266. [PubMed: 9144106]
- Lauterbach EC, Price ST, Wilson AN, Knopik VS, Jackson JG, Kavali CM. Post-stroke major depression: Parkinsonism and thalamocortical systems relations. *Biol Psychiatry*. 1994; 35:681.
- Leentjens AFG, Dujardin K, Marsh L, Martinez-Martin P, Richard IH, Starkstein SE. Symptomatology and markers of anxiety disorders in Parkinson's disease: a cross-sectional study. *Mov Disord*. 2011; 26:484–492. [PubMed: 21312281]
- Lim MM, Murphy AZ, Young LJ. Ventral striatopallidal oxytocin and vasopressin V1a receptors in the monogamous prairie vole (*Microtus ochrogaster*). *J Comp Neurol*. 2004; 468:555–570. [PubMed: 14689486]
- Liu P, Jenkins NA, Copeland NG. A highly efficient recombineering-based method for generating conditional knockout mutations. *Genome Res*. 2003; 13:476–484. [PubMed: 12618378]
- Lowry CA, Moore FL. Regulation of behavioral responses by corticotropin-releasing factor. *Gen Comp Endocrinol*. 2006; 146:19–27. [PubMed: 16426606]
- Madisen L, Zwingman TA, Sunkin SM, Oh SW, Zariwala HA, Gu H, Ng LL, Palmiter RD, Hawrylycz MJ, Jones AR, Lein ES, Zeng H. A robust and high-throughput Cre reporting and characterization system for the whole mouse brain. *Nat Neurosci*. 2010; 13:133–140. [PubMed: 20023653]
- Mallet N, Micklem BR, Henny P, Brown MT, Williams C, Bolam JP, Nakamura KC, Magill PJ. Dichotomous organization of the external globus pallidus. *Neuron*. 2012; 74:1075–1086. [PubMed: 22726837]
- Marchand WR. Cortico-basal ganglia circuitry: a review of key research and implications for functional connectivity studies of mood and anxiety disorders. *Brain Struct Funct*. 2010; 215:73–96. [PubMed: 20938681]
- Miller JM, Vorel SR, Tranguch AJ, Kenny ET, Mazzoni P, van Gorp WG, Kleber HD. Anhedonia after a selective bilateral lesion of the globus pallidus. *Am J Psychiatry*. 2006; 163:786–788. [PubMed: 16648316]
- Mogenson GJ, Jones DL, Yim CY. From motivation to action: functional interface between the limbic system and the motor system. *Prog Neurobiol*. 1980; 14:69–97. [PubMed: 6999537]
- Müller MB, Zimmermann S, Sillaber I, Hagemeyer TP, Deussing JM, Timpl P, Kormann MSD, Droste SK, Kühn R, Johannes MH, Holsboer F, Würst W. Limbic corticotropin-releasing hormone receptor 1 mediates anxiety-related behavior and hormonal adaptation to stress. *Nat Neurosci*. 2003; 6:1100–1107. [PubMed: 12973355]
- Nóbrega-Pereira S, Kessaris N, Du T, Kimura S, Anderson SA, Marín O. Postmitotic Nkx2-1 controls the migration of telencephalic interneurons by direct repression of guidance receptors. *Neuron*. 2008; 59:733–745. [PubMed: 18786357]
- Nusbaum MP, Blitz DM, Marder E. Functional consequences of neuropeptide and small-molecule co-transmission. *Nat Rev Neurosci*. 2017; 18:389–403. [PubMed: 28592905]

- Nuti A, Ceravolo R, Piccinni A, Dell'Agnello G, Bellini G, Gambaccini G, Rossi C, Logi C, Dell'Osso L, Bonuccelli U. Psychiatric comorbidity in a population of Parkinson's disease patients. *Eur J Neurol.* 2004; 11:315–320. [PubMed: 15142224]
- Parent A, Hazrati LN. Functional anatomy of the basal ganglia. II. The place of subthalamic nucleus and external pallidum in basal ganglia circuitry. *Brain Res Brain Res Rev.* 1995; 20(1):128–54. [PubMed: 7711765]
- Parush N, Arkadir D, Nevet A, Morris G, Tishby N, Nelken I, Bergman H. Encoding by response duration in the basal ganglia. *J Neurophysiol.* 2008; 100:3244–3252. [PubMed: 18842956]
- Phelps EA, O'Connor KJ, Gatenby JC, Gore JC, Grillon C, Davis M. Activation of the left amygdala to a cognitive representation of fear. *Nat Neurosci.* 2001; 4:437–441. [PubMed: 11276236]
- Prediger RDS, Matheus FC, Schwarzbald ML, Lima MMS, Vital MABF. Anxiety in Parkinson's disease: a critical review of experimental and clinical studies. *Neuropharmacology.* 2012a; 62:115–124. [PubMed: 21903105]
- Prediger RDS, Matheus FC, Schwarzbald ML, Lima MMS, Vital MABF. Anxiety in Parkinson's disease: a critical review of experimental and clinical studies. *Neuropharmacology.* 2012b; 62:115–124. [PubMed: 21903105]
- Refojo D, Schweizer M, Kuehne C, Ehrenberg S, Thoeniger C, Vogl AM, Dedic N, Schumacher M, von Wolff G, Avrabos C, Touma C, Engblom D, Schutz G, Nave KA, Eder M, Wotjak CT, Sillaber I, Holsboer F, Wurst W, Deussing JM. Glutamatergic and dopaminergic neurons mediate anxiogenic and anxiolytic effects of CRHR1. *Science.* 2011; 333(6051):1903–7. [PubMed: 21885734]
- Saper CB. The central autonomic nervous system: conscious visceral perception and autonomic pattern generation. *Annu Rev Neurosci.* 2002; 25:433–469. [PubMed: 12052916]
- Saunders A, Huang KW, Sabatini BL. Globus Pallidus Externus Neurons Expressing parvalbumin Interconnect the Subthalamic Nucleus and Striatal Interneurons. *PLoS One.* 2016; 11:e0149798. [PubMed: 26905595]
- Siemers ER, Shekhar A, Quaid K, Dickson H. Anxiety and motor performance in Parkinson's disease. *Mov Disord.* 1993; 8:501–506. [PubMed: 8232361]
- Smith GW, Aubry JM, Dellu F, Contarino A, Bilezikjian LM, Gold LH, Chen R, Marchuk Y, Hauser C, Bentley CA, Sawchenko PE, Koob GF, Vale W, Lee KF. Corticotropin releasing factor receptor 1-deficient mice display decreased anxiety, impaired stress response, and aberrant neuroendocrine development. *Neuron.* 1998; 20:1093–1102. [PubMed: 9655498]
- Swanson LW, Sawchenko PE, Rivier J, Vale WW. Organization of ovine corticotropin-releasing factor immunoreactive cells and fibers in the rat brain: an immunohistochemical study. *Neuroendocrinology.* 1983; 36:165–186. [PubMed: 6601247]
- Sztainberg Y, Kuperman Y, Justice N, Chen A. An anxiolytic role for CRF receptor type 1 in the globus pallidus. *J Neurosci.* 2011; 31:17416–17424. [PubMed: 22131403]
- Taniguchi H, He M, Wu P, Kim S, Paik R, Sugino K, Kvitsiani D, Kvitsani D, Fu Y, Lu J, Lin Y, Miyoshi G, Shima Y, Fishell G, Nelson SB, Huang ZJ. A resource of Cre driver lines for genetic targeting of GABAergic neurons in cerebral cortex. *Neuron.* 2011; 71:995–1013. [PubMed: 21943598]
- Tazi A, Swerdlow NR, LeMoal M, Rivier J, Vale W, Koob GF. Behavioral activation by CRF: evidence for the involvement of the ventral forebrain. *Life Sci.* 1987; 41:41–49. [PubMed: 3496511]
- Ugolini G. Specificity of rabies virus as a transneuronal tracer of motor networks: transfer from hypoglossal motoneurons to connected second-order and higher order central nervous system cell groups. *J Comp Neurol.* 1995; 356:457–480. [PubMed: 7642806]
- Vale W, Spiess J, Rivier C, Rivier J. Characterization of a 41-residue ovine hypothalamic peptide that stimulates secretion of corticotropin and beta-endorphin. *Science.* 1981; 213:1394–1397. [PubMed: 6267699]
- Van Pett K, Viau V, Bittencourt JC, Chan RK, Li HY, Arias C, Prins GS, Perrin M, Vale W, Sawchenko PE. Distribution of mRNAs encoding CRF receptors in brain and pituitary of rat and mouse. *J Comp Neurol.* 2000; 428:191–212. [PubMed: 11064361]
- Vine SJ, Moore LJ, Wilson MR. An Integrative Framework of Stress, Attention, and Visuomotor Performance. *Front Psychol.* 2016; 7:1671. [PubMed: 27847484]

- Wamsteeker Cusulin JI, Füzesi T, Watts AG, Bains JS. Characterization of corticotropin-releasing hormone neurons in the paraventricular nucleus of the hypothalamus of Crh-IRES-Cre mutant mice. *PLoS One*. 2013; 8:e64943. [PubMed: 23724107]
- Watabe-Uchida M, Zhu L, Ogawa SK, Vamanrao A, Uchida N. Whole-brain mapping of direct inputs to midbrain dopamine neurons. *Neuron*. 2012; 74:858–873. [PubMed: 22681690]
- Wickersham IR, Lyon DC, Barnard RJO, Mori T, Finke S, Conzelmann K-K, Young JAT, Callaway EM. Monosynaptic restriction of transsynaptic tracing from single, genetically targeted neurons. *Neuron*. 2007; 53:639–647. [PubMed: 17329205]
- Xue Y, Yang Y-T, Liu H-Y, Chen W-F, Chen A-Q, Sheng Q, Chen X-Y, Wang Y, Chen H, Liu H-X, Pang Y-Y, Chen L. Orexin-A increases the activity of globus pallidus neurons in both normal and parkinsonian rats. *Eur J Neurosci*. 2016; 44:2247–2257. [PubMed: 27336845]

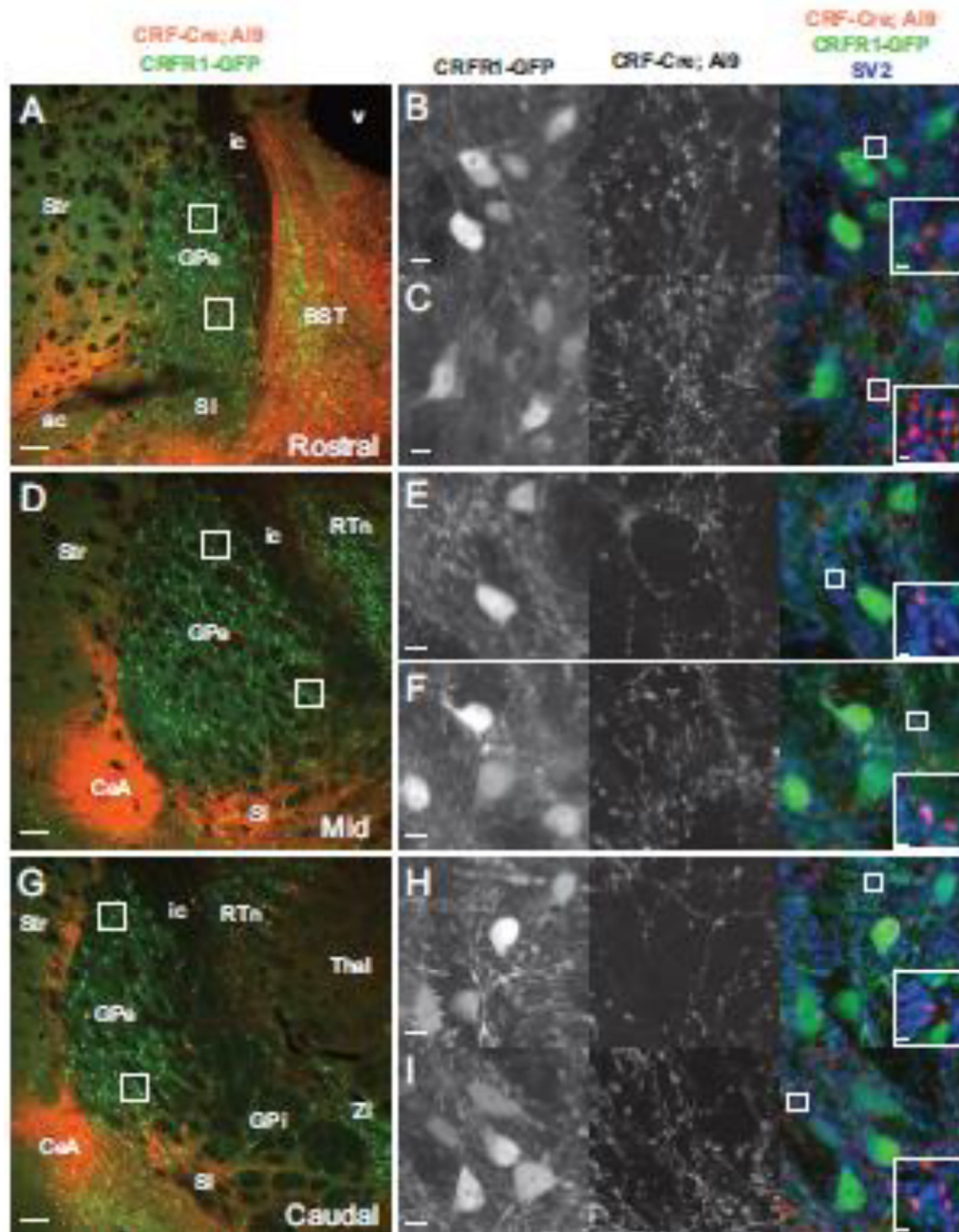


Figure 1. CRF neurons innervate the GPe

Images of the GPe from mice carrying CRFR1-GFP (green, left column and first column on right), CRF-Cre and a Cre dependent ^{td}Tomato reporter (Isl-^{td}Tomato, Ai9, red, left column and second column on right) reveal projections from CRF neurons in close proximity to CRFR1+ neurons. (A) Rostral section at the level of the caudal BST (0.2 mm anterior of bregma). A dorsal closeup (B) and a ventral closeup (C) indicated by boxes in A reveal CRFR1-GFP neurons surrounded by puncta originating from CRF-Cre neurons. The right merged column shows that some of these puncta are positive for the presynaptic marker SV2 (blue), at points of contact between GFP+ dendrites (green) and Tom+ axons (red). (D) A

section of the GPe at the level of the amygdala (0.7mm posterior to bregma). Dorsal (E) and ventral (F) closeups show the innervation of CRFR1-GFP neurons by CRF fibers that in some cases are positive for the presynaptic marker SV2. (G) A caudal section of the GPe (1.22mm posterior to bregma). A dorsal (H) and ventral (I) closeup reveal innervation of CRFR1-GFP neurons by CRF neurons. At all three rostro-caudal levels, CRF presynaptic puncta are more dense in the ventral zone compared to the dorsal zone. A, D, G abbreviations: Str - striatum, ic - internal capsule, v - ventricle, ac - anterior commissure, SI - substantia innominata, BST, Bed Nucleus of the Stria terminalis. Scalebars: A, D, G - 100 μ m, B, C, E, F, H, I - 10 μ m, insets in right column - 1 μ m.

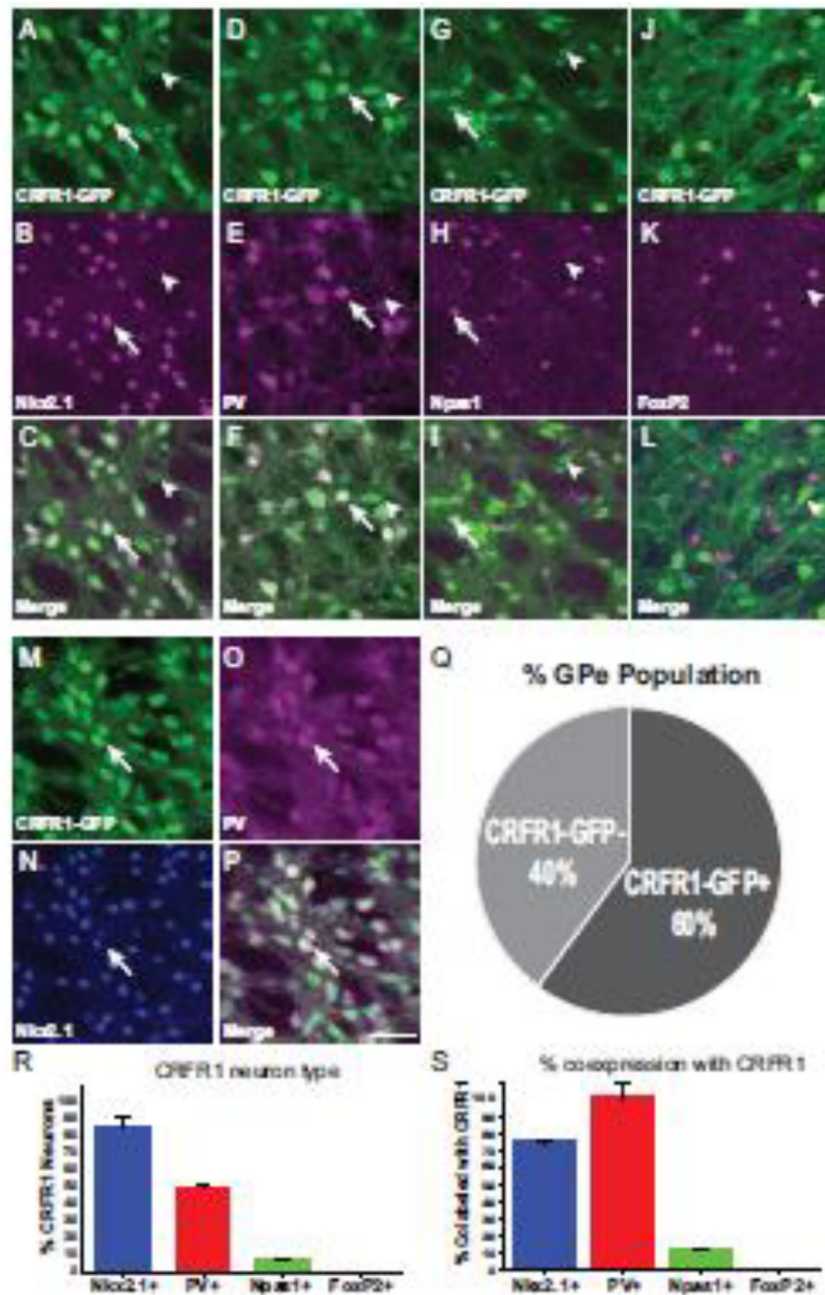


Figure 2. Molecular characterization of CRFR1+ neurons in the GPe
 CRFR1-GFP (green) brain sections were stained for Nkx2.1 (A–C), PV (D–F), Npas1 (G–I), and FoxP2 (J–L; magenta, second row). Merged images show that the majority of CRFR1 positive GPe neurons are also positive for Nkx2.1 (A–C) and PV (D–F; the arrow indicates an example of a double labeled cell, the arrowhead indicates CRFR1-GFP+, marker negative examples). A small number of CRFR1+ neurons are NPas1+ (G–I), and no FoxP2 neurons express CRFR1 (J–L). (M–P) PV (magenta) is expressed by a subset of CRFR1+ (green) Nkx2.1+ (blue) neurons. The arrow indicates an example of a triple labeled neuron. (Q) Quantification of the proportion of total GPe neurons that are CRFR1-GFP+ determined by

NeuN staining. (R) Quantification of the percent overlap of each molecular marker with GFP. (S) Quantification of the percent of each defined cell type that co-expresses CRFR1-GFP. Scale bar = 50 μ m

Author Manuscript

Author Manuscript

Author Manuscript

Author Manuscript

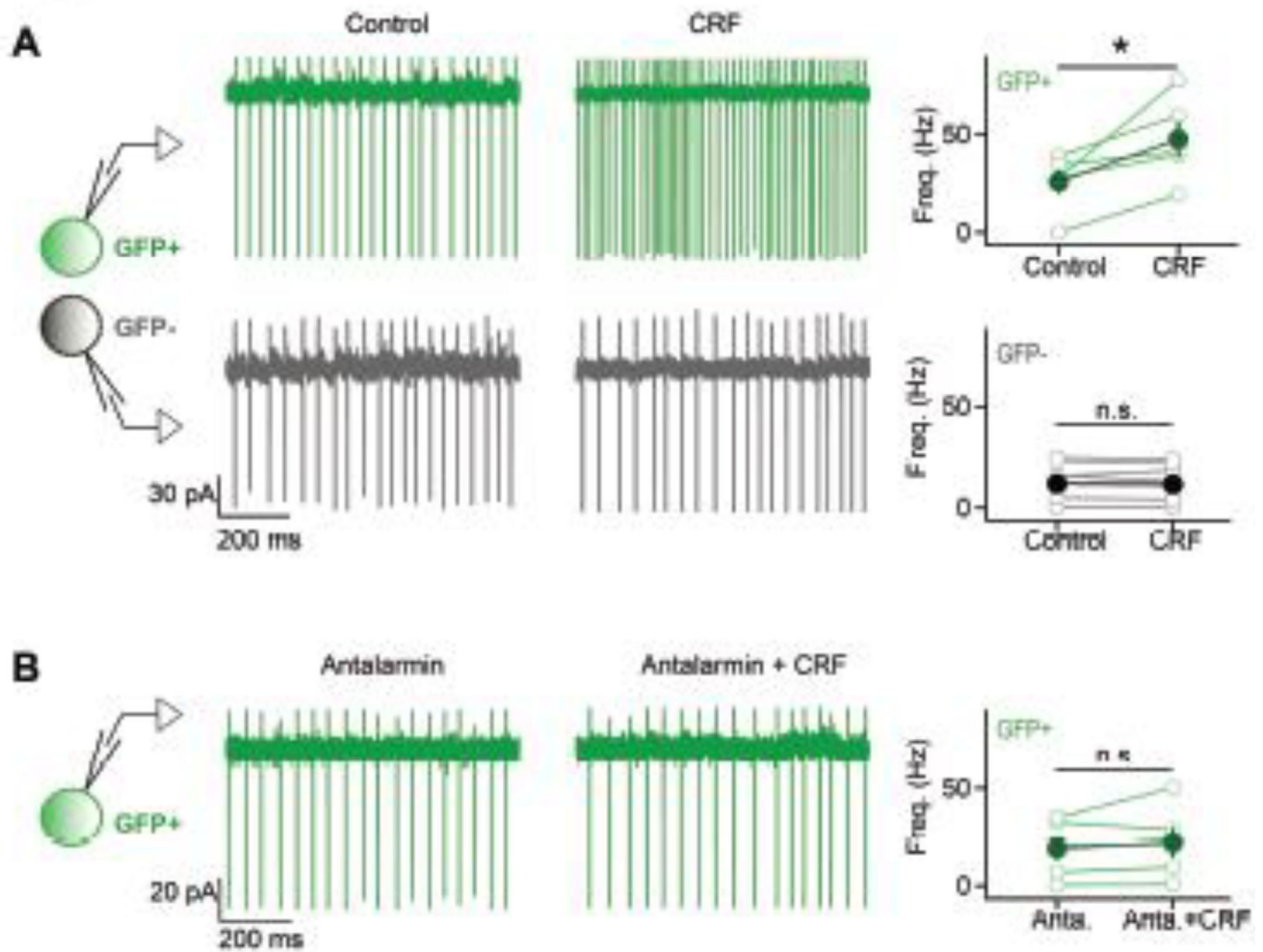


Figure 3. CRF increases firing rates in CRFR1 neurons

(A) Simultaneous loose-patch voltage clamp recordings from neighboring GFP+ (green traces) and GFP- (grey traces) neurons (<100 μm intersomatic distance). Bath application of 30 nM CRF led to an increase in firing in the GFP+ cell but not in the GFP- cell. Right, Quantification of CRF-induced changes in firing rates of GFP+ (top) and GFP- neurons (bottom). All data were recorded from mixed pairs ($n = 5$ pairs). (B) Representative loose-patch recording from a GFP+ cell in the presence of 1 μM Antalarmin in the bath solution. Bath application of 30 nM CRF did not lead to an increase in firing frequency. Right, Quantification of CRF-induced changes in firing rates of GFP+ neurons recorded in the presence of Antalarmin. $n=5$ neurons.

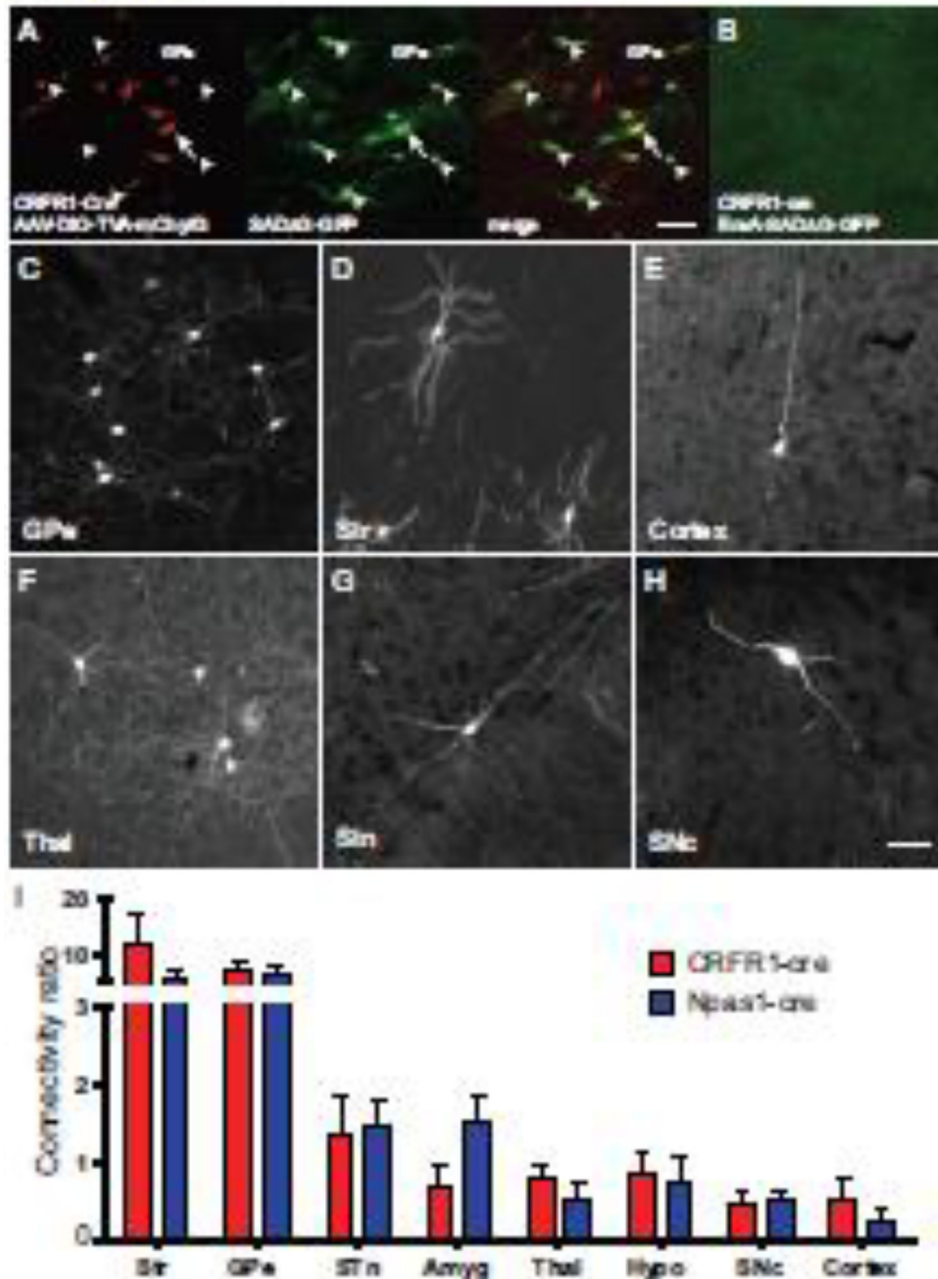


Figure 4. Rabies viral tracing of CRFR1+ and Npas1+ GPe neurons

(A) Injection of AAV helper viruses encoding Cre-dependent TVA-mCherry (red) and G allow for infection by EnvA pseudotyped, G-deleted rabies virus that expresses GFP (SAD-G-GFP, green). The merged image shows a starter cell that expresses both the helper and the rabies viruses (yellow, arrow) surrounded by neurons expressing GFP only (green, arrowheads) which have been transsynaptically infected via a synapse with a starter cell. Scalebar = 50µm. (B) Injection of pseudotyped rabies virus in animals without helper virus injection results in no infection, and no GFP expression. (C–H) Patterns of monosynaptic retrograde infection were broadly similar in CRFR1-cre and Npas1-cre experiments. The

most presynaptic neurons were located in the GPe (C) and the Striatum (Str; D). We also observed neurons in the Cortex (E), Thalamus (Thal; F), Sub-thalamic nucleus (STN; G) and Substantia Nigra pars compacta (SNc; H). Quantification of tracing data reveals that projection patterns to CRFR1+ GPe neurons (red) and Npas1+ GPe neurons (blue) are broadly similar across many brain regions. n=3 per genotype.

Author Manuscript

Author Manuscript

Author Manuscript

Author Manuscript

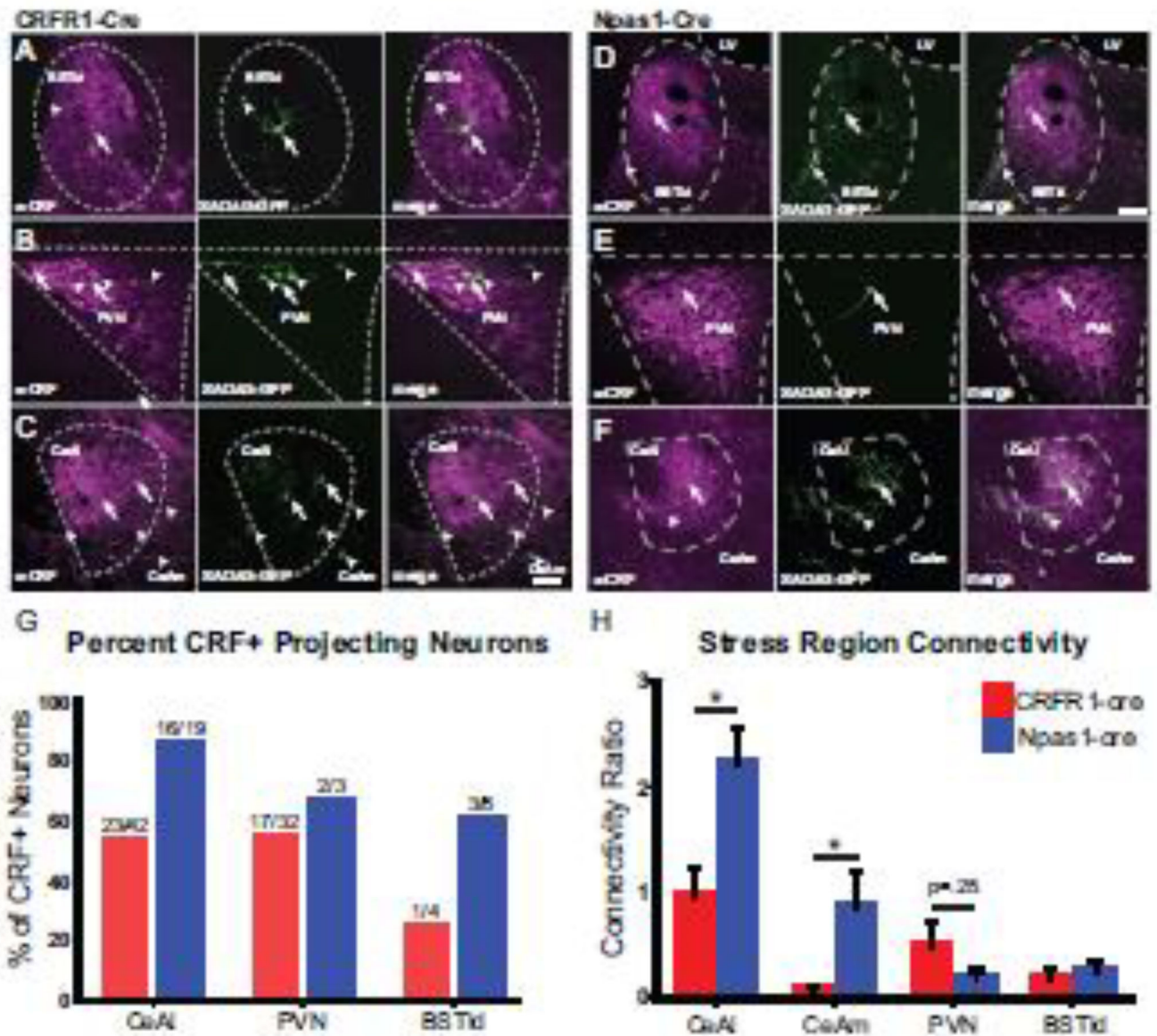


Figure 5. CRF neurons monosynaptically project to CRFR1+ and Npas1+ GPe neurons
 In animals traced from CRFR1+ neurons in the GPe (A–C) we found monosynaptically connected neurons in the lateral-dorsal Bed Nucleus of the Stria Terminalis (BSTld; A), the Paraventricular nucleus of the hypothalamus (PVN; B) and the Central Nucleus of the amygdala (CeA; C). Staining for CRF (second column; green) reveals that a portion of GPe projecting neurons are CRF positive. Arrows indicate CRF+ GPe projecting neurons, arrowheads indicate CRF– GPe projecting neurons. In Npas1+ GPe tracing experiments we also saw monosynaptically projecting neurons in the BSTld (D), PVN (E) and CeA (F). Staining of sections for CRF (green) show that some of these neurons contain CRF peptide (Magenta, arrows), while other neurons do not (arrowheads). A–L, Scalebar = 50µm. (H) Quantification of the percentage of neurons that are CRF positive in each stress-related nucleus. Of the sections that were stained for CRF, we found the ratio of neurons listed above each bar were positive for CRF peptide. (G) Quantification of the connectivity

between key stress responsive nuclei and CRFR1 neurons (red) and Npas1 neurons (blue) in the GPe. The CeAl (lateral division of the CeA) and CeAm (medial division of the CeA) make more connections with Npas1+ neurons than with CRFR1+ neurons. * = $p < 0.05$, $n = 3$ per genotype. Connectivity ratio is the number of neurons present in each nucleus per starter neuron.